energies

MDPI

Article

Integrated One-Dimensional and CFD Modelling of a Radiant Platen Superheater in Industrial Boiler Conditions

Michalina Kurkus-Gruszecka [1], Aleksandra Dzido [1], Adrianna Kwiecień [1], Patrycja Paśniewska [1], Jolanta Ziaja [2] and Piotr Krawczyk [1,*]

[1] Faculty of Power and Aeronautical Engineering, Warsaw University of Technology, Nowowiejska 21/25, 00-665 Warsaw, Poland; michalina.gruszecka@pw.edu.pl (M.K.-G.); patpasniewska@gmail.com (P.P.)
[2] Grupa Kapitałowa Polimex Mostostal, Al. Jana Pawła II 12, 00-124 Warsaw, Poland; jolanta.ziaja@polimex.pl
* Correspondence: piotr.krawczyk@pw.edu.pl

Abstract

Accurate prediction of thermal and flow phenomena in radiant platen steam superheaters is essential for ensuring the safe and efficient operation of industrial steam boilers. This task remains challenging due to the strong coupling between radiative heat transfer in the boiler, flue-gas aerodynamics, and steam-side flow conditions. This paper presents a novel multi-scale modelling framework that integrates a 1D steam-side model with both boiler-scale and local CFD simulations in an iterative manner. The developed approach combines three complementary components: (i) a 1D thermo-hydraulic model of a selected platen implemented in Aspen HYSYS, (ii) a full-scale CFD model of the boiler first pass for determining gas-side thermal conditions, and (iii) a conjugate CFD model of a superheater fragment for detailed analysis of flue gas–steam heat transfer and tube wall temperatures. The models are coupled through the exchange of boundary conditions, enabling consistent representation of both steam-side and gas-side phenomena. The proposed hybrid approach enables analysis of the heat exchanger's operating parameters, such as metal temperatures, steam temperatures, flue-gas temperatures, non-uniform steam flow distribution in the heat exchanger, and pressure drops across the heat exchanger. The 1D model captures flow maldistribution between tubes, while CFD simulations provide detailed insight into boiler temperature distribution and local heat-transfer conditions. The proposed methodology significantly improves the balance between computational cost and modelling accuracy compared to standalone approaches. It offers a flexible and robust tool for analysing superheater operation under varying load conditions and can support design optimisation, operational diagnostics, and future extensions toward transient analysis and lifetime assessment.

Keywords: radiant platen superheater; thermal-flow modelling; CFD modelling; one-dimensional modelling; heat transfer; boiler simulation

Check for updates

Academic Editor: Mahmoud Bourouis

Received: 25 October 2026
Revised: 19 November 2026
Accepted: 24 November 2026
Published: 27 November 2026

Copyright: © 2026 by the authors. Licensee MDPI, Basel, Switzerland. This article is an open access article distributed under the terms and conditions of the Creative Commons Attribution (CC BY) license.

1. Introduction

The accurate prediction of thermal performance in radiant platen superheaters remains a persistent challenge in industrial boiler analysis due to the complex interaction of radiative heat transfer, flue-gas flow, and steam-side conditions. Full CFD approaches, although detailed (full temperature and heat flux profiles are available), are computationally expensive and often impractical for iterative design or operational studies [1]. What is more, detailed modelling of such a huge structure as a combustion chamber, with more detailed components such as complex structures of steam superheaters or reheaters, increases computational time and may cause numerical instabilities due to high pressure

gradients through walls. These barriers make combined flue-gas-side and water–steam-side calculations challenging. The other approach is 1D modelling, which offers computational efficiency but relies on strong simplifications of the furnace radiation field and cannot provide detailed distributions of key parameters like temperature or heat transfer. Such distributions may be crucial because, in platen superheaters, the problem of uneven wall temperature distribution is significant and may influence the mechanical behaviour of the material. Thermal stresses might cause fissures in boiler tubes, which are critical components in estimating the availability and efficiency of the plant [2]. Thus, the most severe wall temperature should be considered. The temperature differences in the superheater walls are influenced by two factors: flow maldistribution and non-uniform heat flux distribution.

The former is induced by reduced coolant mass flow: density differences caused directly by heat flux differences and pressure losses due to different tube shapes and lengths [3]. Boiler pressure elements such as platen and pendant heaters, especially low-pressure ones, are liable to overheating caused by lower steam flow and poor dissipation conditions [4]. For analysing the flow impact on wall temperature, the Finite Element and Finite Volume Methods are used.

Madejski and Tyler [5] conducted thermal stress calculations in the CFB boiler superheater during transients. CFD (Computational Fluid Dynamics) analysis was used for calculating working medium parameters and wall temperature distribution in double omega tubes using STAR CCM+ software London: Computational Dynamics Ltd. (London, UK); 2011. The temperature of the fluidised bed was not modelled and was assumed to be constant along the combustion chamber height and equal to the measurements.

The highest wall temperature was found at the corners of the omega tubes, which may cause severe corrosion failures. For the lower load, the steam temperature increase was higher than for 100% load.

In [6], steam flow parameters and wall temperature calculations obtained with the Control Volume-based Finite Element Method were compared to the CFD simulation results. The proposed model reduces the computational resources needed for the steady-state flow calculations in tubes with complicated cross-sections compared to the CFD simulations.

The uneven heat flux distribution is caused by aerodynamics and combustion process complexity in the furnace. The gas temperature in the lower part of the superheater is high, which dominates heat transfer by radiation, with a lower convection influence. Heat flux reaches the highest values in the lower part of the superheater, causing increased wall temperature in this region [3]. Edge et al. [7] carried out a complex CFD analysis of furnace temperature distribution.

In this approach, 3D modelling considering flow patterns and load-dependent temperature distribution in the domain of the combustion chamber, superheater and reheater regions is necessary [4]. Shen et al. [8] and Xu et al. [9] focused on combustion process modelling.

For the coupled analysis of the flue gas and working medium, simplifications are necessary to reduce the computing costs. An example of such a method is a porosity concept explained by Prieto [10] and applied to a 350 MW power plant model [11].

Jin et al. [3] proposed a coupled 3D combustion process model to estimate the uneven heat flux distribution with the 1D tube flow to properly calculate steam temperature. The results were consistent with the experimental measurements of wall temperature at the steam outlet. Using CFD modelling, the authors showed the influence of heat flux on steam temperature and coolant mass flow. The uneven heat flux distribution in the furnace, together with the tube length differences, caused steam and wall temperature deviations both between panels and specific tubes constituting them.

Modliński et al. [4] conducted furnace CFD modelling with MHEM (Macro Heat Exchanger Model) to reduce the computation costs. To model flow parameters in the second-

stage reheater tubes, a 1D HPFM (Heated Pipe Flow Model) was used. In the analysed furnace, restricting orifices were installed to reduce the flow in tubes exposed to lower heat flux. The simulation results were confirmed by the thermocouple measurements. The simulation showed the dependency of heat flux on the load, emphasising the complexity of choosing the proper placement of the orifices. A brief description of the furnace simulations (OP-380 and OP-430) is provided in [12]. Another combined 3D CFD and 1D boiler model for the Youngheung Power Plant Units 1 and 2 was proposed and validated by Park et al. [13].

Additionally, stress and strain investigations can be found in the literature. Duda [14] proposed an algorithm that enables stress and strain distribution calculation based on the measurements of the temperature at easily accessible points on the outer diameter of the pressure component. Fu et al. [15] measured and investigated the temperature, heat flux, stress and strain parameters in a scaled-down model of a furnace.

Even though online measurement of wall temperature became standard many years ago, overheating observations may already be associated with material damage [4]. Heat transfer and fluid dynamics modelling play a great role in estimating the most severe parameter of the tube walls.

The load of the boiler strongly influences the highest wall temperature and steam temperature gradients. Decreased steam flow for lower loads causes higher wall temperature despite the reduced heat flux from the combustion chamber [3]. Thus, usually simulations are conducted for two loads: 100% and 50% [3] or 60% [4,5]. Laubscher and Rousseau [16] conducted CFD simulations for 99%, 81% and 60.5% boiler loads and compared the results with the experimental data.

Additionally, an increase in wall temperature may be caused by the increased heat-transfer resistance. The impact of ash fouling on the heat-transfer coefficient in the heat exchanger was analysed by Vessakosol and Charoesunk [17] using the Control Volume Finite Element Method. Song et al. [18] investigated the process of ash deposition in a circulating fluidised bed type boiler.

While previous studies have demonstrated the benefits of coupling CFD simulations with one-dimensional steam-side models, the present work develops a multi-scale modelling framework in which a one-dimensional superheater model is iteratively coupled with boiler-scale CFD simulations and complemented by a detailed three-dimensional conjugate heat-transfer model of the SH2 fragment. The one-dimensional model resolves steam flow distribution among individual tubes, while the boiler-scale CFD model provides spatially resolved flue-gas conditions. Importantly, the detailed SH2 model explicitly resolves three coupled three-dimensional computational domains representing the flue gas, the solid tube walls, and the steam flowing inside the tubes. This approach enables the analysis of local tube metal temperature distributions while accounting for non-uniform gas-side thermal loading, heat conduction through the tube walls, and tube-specific steam cooling conditions. By combining different levels of modelling detail, the proposed framework provides a practical tool for investigating the thermal and hydraulic behaviour of radiant platen superheaters under industrial boiler operating conditions.

2. Methods

2.1. Overall Modelling Strategy

The present work develops and applies a multi-scale modelling framework for a radiant platen superheater (denoted SH2) installed in a large industrial steam boiler. The main objective is to numerically reproduce the thermo-hydraulic behaviour and operating conditions of the superheater tubes for a range of boiler loads, with particular attention to nominal and minimum-load operation.

To achieve this, three complementary numerical models are combined:

1. A one-dimensional hydraulic and thermal model of a selected platen of SH2, implemented in Aspen HYSYS, which represents the steam flow in individual coils and the associated pressure losses and heat absorption.
2. A full-scale CFD model of the first pass of the boiler, used to calculate three-dimensional flow and temperature fields of the flue gas and to determine the thermal conditions in the region where the platen superheater is located.
3. A detailed CFD model of a fragment of SH2, including selected platens together with the surrounding flue-gas region and the tube walls, which enables a conjugate heat-transfer analysis and the prediction of tube metal temperature distributions.

The models are coupled through boundary conditions: the boiler-scale CFD provides gas-side temperature and heat-transfer characteristics in the superheater region, while the 1D model supplies steam-side mass flow rates and inlet conditions to the detailed SH2 CFD model (Figure 1). In this way, a consistent description of the operating state of the superheater is obtained for the different boiler loads considered. The one-dimensional model was developed using Aspen HYSYS v11 (AspenTech), while the boiler-scale and local superheater CFD simulations were performed using ANSYS Fluent 2021 and ANSYS CFX 2021 (ANSYS, Inc., Canonsburg, PA, USA), respectively. All software packages were used under research licenses.

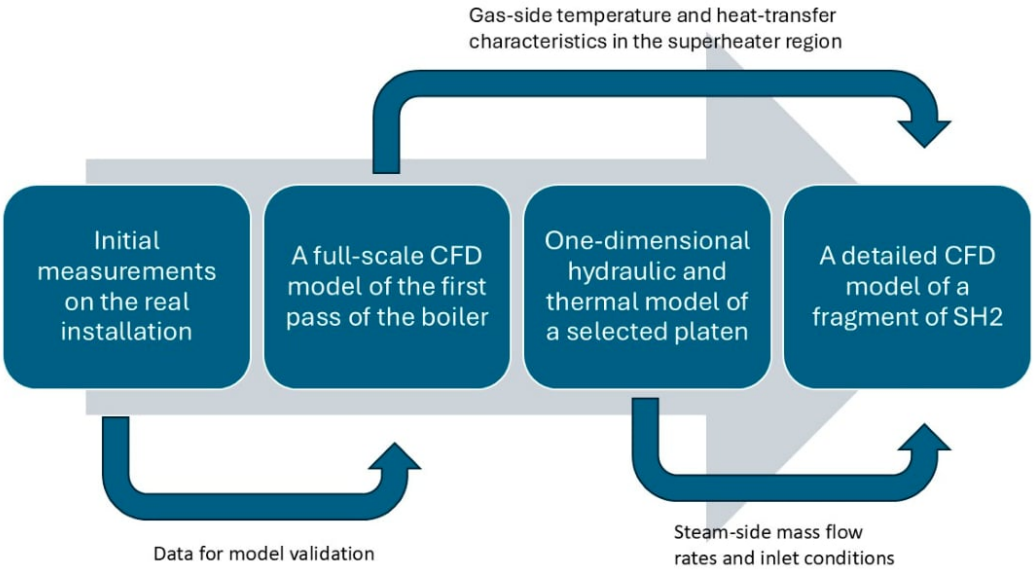


Figure 1. Scheme of the modelling approach and data sharing between the implemented models.

2.2. One-Dimensional Steam Flow Model

2.2.1. General Model

One-dimensional (1D) steam pipe modelling represents a simplified yet rigorous approach to simulating flow behaviour in piping networks by discretising transport phenomena along a single spatial dimension. The model fundamentally solves momentum, energy, and mass balance equations [19] to predict how pressurised steam flows through conduits while accounting for thermodynamic state changes. Property calculations rely on ASME steam tables [20], with two principal thermodynamic packages available: the ASME Steam Package, which operates across a broad range spanning pressures up to 15,000 PSIA and temperatures from 32 °F to 1500 °F, and the NBS Steam Package, which provides enhanced accuracy near the critical point for systems experiencing high-pressure and near-critical conditions [21,22].

The flow through the valves was calculated according to (1) [23].

$$\dot{m} = k\sqrt{\Delta p} \quad (1)$$

$\dot{m}$—mass flow [kg/s], k—coefficient representing the inverse of flow resistance (conductivity) [$\sqrt{\text{kg·m}}$], and Δp—pressure drop [Pa]

The mass flow rate depends on the inlet pressure (p_{in}), outlet pressure (p_{out}), and the C_V coefficient corresponding to the inverse of flow resistance (2).

$$\dot{m} = f(p_{in}, p_{out}, C_V) \quad (2)$$

The Pipe Segment model discretises the piping system to calculate pressure gradients resulting from frictional losses and elevation changes, while simultaneously tracking enthalpic distributions and vapour–liquid quality ratios throughout the pipeline length. Heat-transfer interactions across pipe boundaries are incorporated through specified boundary conditions, and the formulation accounts for dynamic effects including fluid acceleration and static head contributions. This computational framework enables rapid system-level analysis without necessitating computationally expensive three-dimensional computational fluid dynamics simulations, thereby achieving practical engineering accuracy while preserving computational efficiency for design and optimisation studies [24].

2.2.2. Model Implementation

The one-dimensional model represents the thermo-hydraulic behaviour of a single platen of SH2 consisting of 16 parallel tubes (coils). The geometry of this platen was reconstructed based on design documentation so that the actual flow paths and tube lengths could be reproduced in the numerical model.

To capture axial variations in thermal loading along the tubes, each coil was divided into segments:

- Tube no. 1 (outer tube): 3 segments (vertical inlet leg, horizontal section, vertical outlet leg);
- Tubes no. 2–16: 5 segments per tube, defined according to the coil layout and bend positions.

The adopted segmentation of tubes 2–16 is illustrated in Figure 2. This segmentation provides a flexible framework for assigning spatially varying heat input along the tubes, based on boiler heat balances and on the authors' own CFD predictions of furnace conditions (see Section 2.3). The resulting 1D model thus combines realistic geometry with a sufficiently detailed description of heat absorption.

The hydraulic network of the platen was implemented in Aspen HYSYS using standard unit operations arranged to replicate the actual tube configuration (Figure 3):

- Pipe elements were used for straight tube sections and bends;
- TEE elements were used at junctions where the inlet steam flow splits between individual coils;
- Valve elements were introduced to model local pressure losses associated with steam entry into and exit from each tube.

For each straight section and bend, the equivalent length, inner diameter and roughness were specified based on design data. Geodetic height differences between tubes were neglected, as they are identical for all coils and do not influence the relative distribution of flow in the model.

Water and steam properties are described using the ASME Steam property package, which ensures a thermodynamically consistent representation of the working fluid over the full range of pressures and temperatures considered.

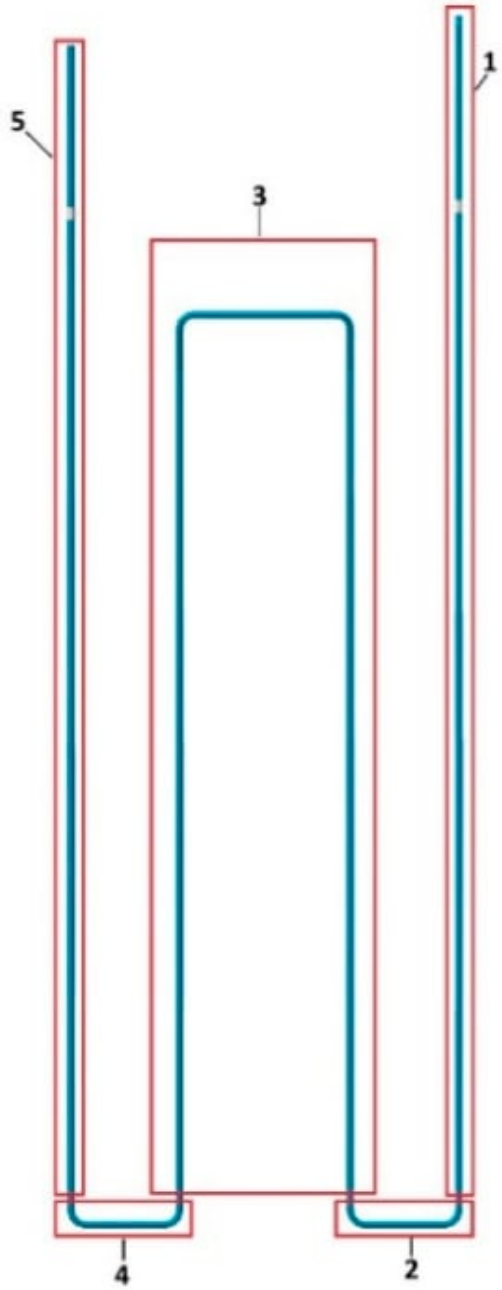


Figure 2. Layout of tubes 2–16 in the analysed platen and their division into five axial segments used in the one-dimensional model.

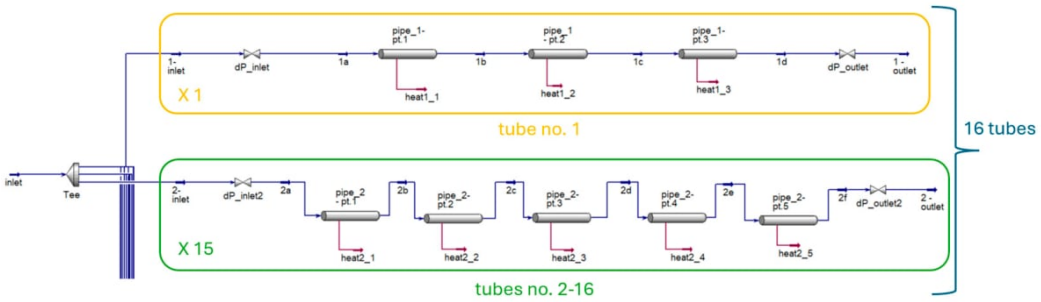


Figure 3. One-dimensional hydraulic and thermal model of the selected platen implemented in Aspen HYSYS.

2.2.3. Iterative Solution Procedure of 1D Model

For a given operating condition, the one-dimensional (1D) model of the platen superheater was solved using an iterative procedure developed by the authors. The model calculations were performed for prescribed boundary and operating conditions, including the total steam mass flow rate entering the platen, the inlet steam pressure and temperature, and the total heat absorbed by the platen with its specified distribution among tubes and segments.

The solution proceeds as follows:

1. An initial, uniform distribution of steam mass flow rate among all coils is assumed.
2. For this assumed distribution, Aspen HYSYS is used to calculate the pressure drop in each tube, considering both frictional and local losses.
3. Based on the calculated pressure drops, the steam mass flow rates in the tubes are updated so as to approach a condition of equal pressure drop across all coils.
4. Steps 2–3 are repeated until the pressure drops converge within a prescribed tolerance.

After convergence, the model provides the steam mass flow rate, pressure drop, inlet and outlet conditions, and segment-wise thermodynamic states for each tube. These results constitute the steam-side input to the more detailed CFD analysis of the superheater fragment (see Section 2.4).

2.3. Numerical Model of the Boiler

2.3.1. Computational Domain and Mesh

To provide gas-side boundary conditions for the superheater, a three-dimensional CFD model of the first pass of the boiler was developed. The domain covers:

- The furnace chamber with explicitly modelled burners for the main fuel;
- Start-up burners with their cooling air systems;
- Staged air nozzles (SOFA);
- The radiant and convective surfaces of SH2 and neighbouring heat exchangers.

The overall computational domain, together with the location of the platen superheater SH2 and an enlarged view of the burner region, is shown in Figure 4. The furnace chamber has an approximately square cross-section of 9 × 9 m, while the SH2 platen superheater has a height of approximately 10 m.

The real boiler geometry was represented in a simplified form to keep the mesh size at a practical level. Membrane walls were modelled as flat surfaces, selected internal pipelines were omitted, and the ash hopper and roof were included only approximately. Partition superheaters were represented as plate-like elements with a thickness corresponding to the tube outside diameter, without explicitly resolving the gaps between tubes. Local fouling deposits and openings in the waterwall system, such as manholes or measurement ports, were not included.

In the burner zone, only the outlet sections of individual nozzles were explicitly modelled, with their final shapes preserved but without small internal details. All nozzles were assumed to inject flow horizontally, without tilt. Secondary air nozzles were represented in a simplified way, and the model also includes over-fire air nozzles and ignition burner nozzles with their cooling air, so that their influence on the flow pattern in the furnace is captured.

The superheater coils are represented as plate-like surfaces with a thickness equal to the external tube diameter. This modelling choice offers a compromise between geometric detail and computational efficiency and is sufficient for obtaining realistic gas-side temperature and heat-transfer conditions in the region of SH2.

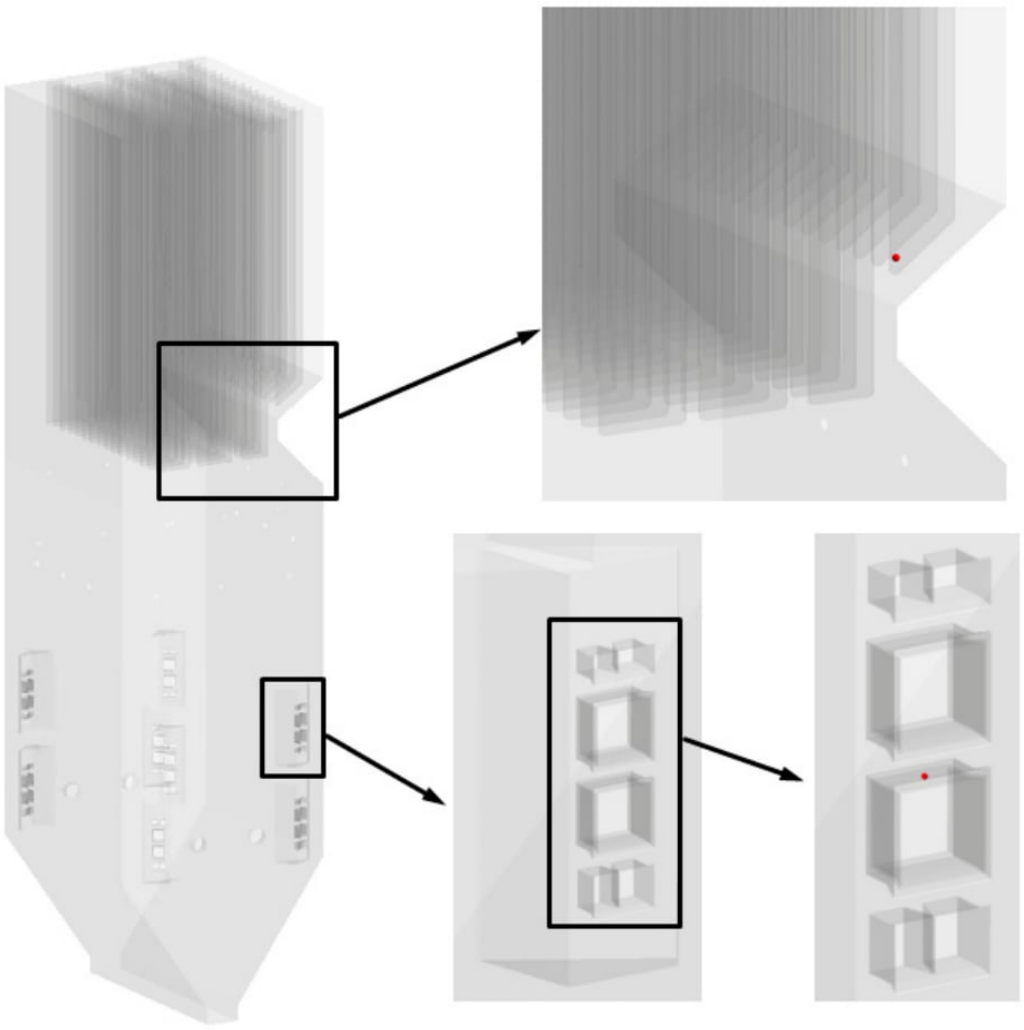


Figure 4. Computational domain of the boiler CFD model, showing the first pass, the location of the platen superheater SH2 and an enlarged view of the burner region.

The computational mesh consists of polyhedral cells. During the model setup, five alternative meshes of different overall density were tested. In all cases, local refinement was applied in the burner belt region and in the vicinity of key components, in particular around the fuel and air nozzles and the partition heat exchangers in the upper part of the first pass. Near the boiler heat-transfer surfaces, inflation layers were introduced so that the non-dimensional wall distance y^+ remained below about 300, consistent with the use of wall functions. The final mesh adopted for the simulations contains approximately 13 million cells, which was found to offer an appropriate compromise between accuracy and computational cost. The overall view of the resulting mesh is shown in Figure 5.

2.3.2. Boundary Conditions and Operating Points

Boundary conditions for the CFD simulations were derived from boiler balance data and fuel analysis. In the present work, the results of the boiler CFD model are presented for the nominal operating point corresponding to 100% load.

For this operating point, the following data were used:

- Flow rates, temperatures and compositions at the inlets for primary, secondary and tertiary air streams;
- Fuel feed rates and fuel characteristics;
- Outlet pressure and global heat balance.

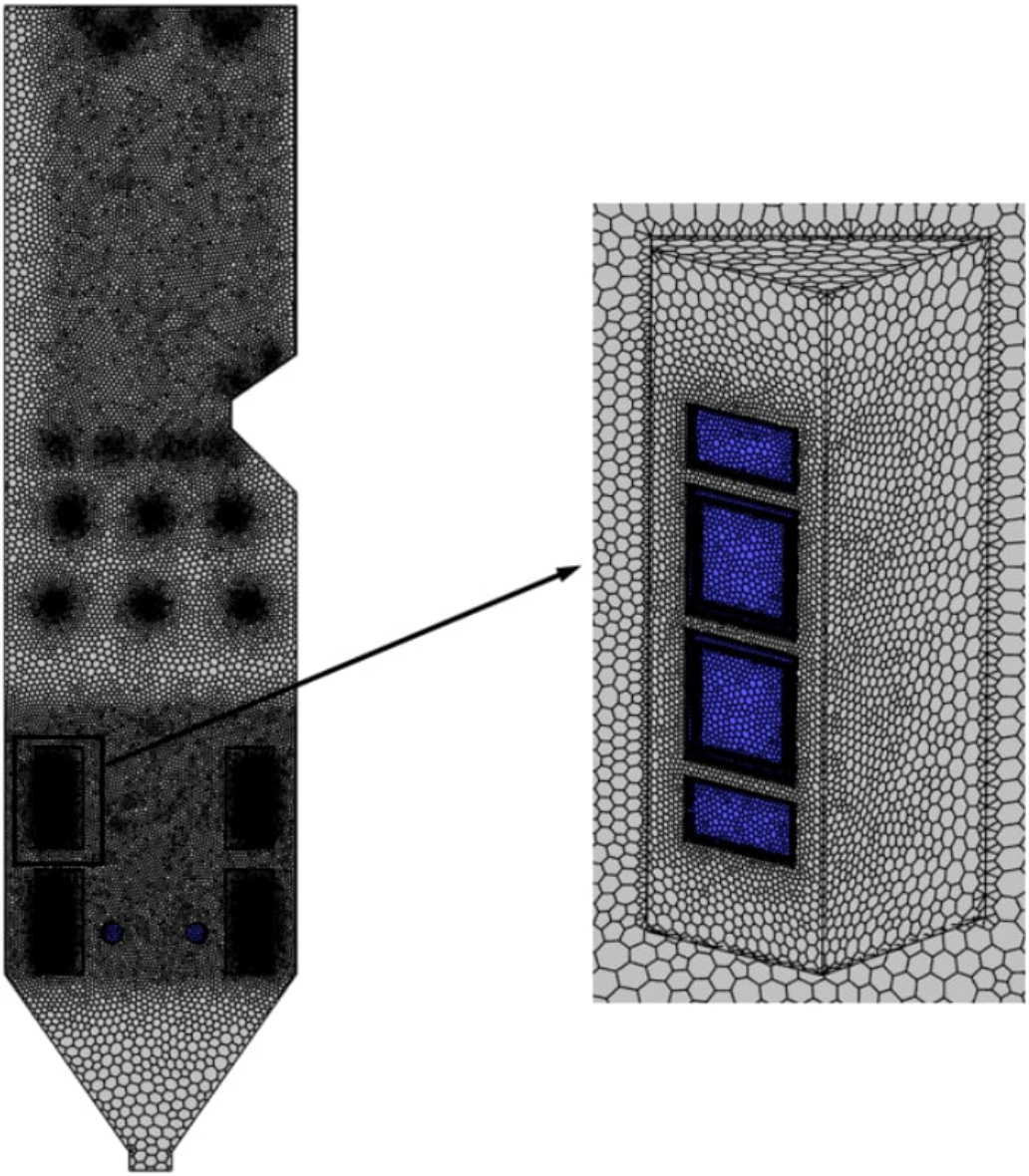


Figure 5. Polyhedral computational mesh of the boiler CFD domain with an enlarged view of the burner region.

Burner and staged-air inlets were defined using velocity and temperature profiles consistent with the plant data. The primary and secondary air mass flow rates supplied to each burner were approximately 4.80 kg/s and 2.40 kg/s, respectively.

This setup enables the CFD model to reproduce the main features of the combustion process and the subsequent flue-gas flow in the first pass of the boiler.

2.3.3. Physical and Numerical Models Used in the Boiler CFD Simulations

The boiler-scale CFD simulations were performed in ANSYS Fluent using a finite-volume framework to solve the Reynolds-averaged conservation equations for mass, momentum and energy, together with species transport equations for the individual gaseous components. Gravity was included in the momentum equations so that buoyancy effects associated with strong temperature- and composition-dependent density variations in the furnace could be represented. This is particularly important for natural convection and stratification of the hot flue gases.

Turbulence in the gas phase was modelled using the realisable k–ε model [25] with standard wall functions and default model coefficients. This model is widely used for the numerical analysis of flows and combustion processes in power boiler furnaces [26–29] and offers a good compromise between robustness, accuracy and computational cost. Wall-adjacent cells were chosen such that the non-dimensional wall distance y^+ is compatible with the use of wall functions.

Radiative heat transfer between the hot flue gases and the furnace walls, as well as the heat exchanger surfaces, was represented using the Discrete Ordinates (DO) radiation model [30–32]. The radiative transfer equation was solved for a set of discrete directions defined by a standard angular discretisation, which provides a sufficient resolution of the radiative intensity field for engineering applications. The absorption coefficient of the gas mixture was evaluated as a function of the concentration of major participating species, primarily CO_2 and H_2O, using correlations recommended for combustion gases [33]. Scattering was neglected, and the walls were treated as grey, diffusely emitting and reflecting surfaces, with emissivity coefficients ranging from 0.7 to 0.9.

Chemical reactions in the gas phase were described using the Eddy-Dissipation combustion model [34], in which the reaction rate is controlled by the turbulent mixing of reactants. The properties of pulverised coal used in the CFD simulations, including proximate analysis, elemental composition, and lower heating value, are summarised in Table 1. The particle size distribution was represented using the Rosin–Rammler model, with the corresponding parameters also provided in Table 1.

Table 1. Pulverised coal properties and Rosin–Rammler particle size distribution parameters adopted in the CFD simulations.

Parameter	Value	Unit
Proximate analysis		
Volatile matter	31.82	wt.%
Fixed carbon	43.49	wt.%
Ash	24.69	wt.%
Moisture	0.00	wt.%
Elemental composition		
Carbon (C)	81.52	wt.%
Hydrogen (H)	4.39	wt.%
Oxygen (O)	10.59	wt.%
Nitrogen (N)	1.84	wt.%
Sulfur (S)	1.65	wt.%
Fuel properties		
Lower heating value (LHV)	21,348.49	kJ/kg
Rosin–Rammler distribution		
Model coefficient, b	0.0128134	—
Spread parameter, n	1.11063	—
Mean diameter parameter	50.54	µm
Minimum particle diameter	10	µm
Maximum particle diameter	200	µm

Note: The elemental composition is normalised to the sum of C, H, O, N, and S, excluding ash. The zero moisture content refers to the dry coal particles introduced into the CFD domain.

Volatile release and char oxidation were represented by global reaction steps consistent with the eddy-dissipation formulation.

The solid fuel was introduced into the computational domain as a discrete particulate phase. Pulverised coal was modelled as a stream of spherical particles injected at the outlets of the fuel nozzles in the burner belt. A Rosin–Rammler particle size distribution [35,36]

was imposed to reflect the spread of particle diameters observed in measurements of milled coal from the boiler mills. Particle trajectories were computed in a Lagrangian frame of reference [37], taking into account drag and gravity; heat and mass transfer between the particles and the surrounding gas were coupled through the source terms in the gas-phase equations.

In the present modelling approach, it was assumed that the moisture contained in the pulverised coal evaporates into the carrier air in the fuel ducts upstream of the burner outlets. As a result, the coal particles injected into the furnace are treated as dry, while the corresponding amount of water vapour is added to the primary air streams at the burner inlets.

Surface temperatures of the boiler heat-transfer elements (membrane walls, superheaters and other heating surfaces) were prescribed on the basis of plant data and calculations for the water–steam cycle. A temperature boundary condition was imposed on the evaporator waterwalls. The wall temperature was assumed to be approximately 20 K higher than the steam saturation temperature of 613 K, resulting in a prescribed wall temperature of approximately 633 K. In this way, the CFD model reproduces the thermal boundary conditions experienced by the gas phase at the analysed operating points.

For the pressure–velocity coupling, the Coupled algorithm was employed [38]. Spatial discretisation of the convective terms in the momentum, energy and species equations used second-order upwind schemes, while diffusive terms were treated with second-order central differencing. This combination ensures a reasonable balance between numerical stability and solution accuracy for the strongly convective, high-Reynolds-number flows present in the furnace.

2.4. CFD Model of the SH2 Fragment

2.4.1. Computational Domain and Mesh

To resolve the thermal behaviour of individual tubes in more detail, a CFD model of a fragment of SH2 was developed. This model includes two adjacent platens of SH2, the flue-gas region surrounding and between these platens, the internal flow passages of the tubes, and the solid tube walls. A schematic view of the computational domain is shown in Figure 6.

In contrast to the boiler-scale model, the SH2 fragment model treats the flue gas, tube metal and steam as three coupled media in a conjugate heat-transfer simulation. The computational mesh, shown in Figure 7, is a hybrid mesh consisting of approximately 87 million cells, which allows the resolution of boundary layers on both the gas and steam sides and an accurate representation of temperature gradients within the tube walls.

2.4.2. Boundary Conditions and Coupling Strategy

The SH2 fragment model is coupled with the other components of the modelling framework through its boundary conditions:

- Flue-gas inlet conditions (velocity and temperature) are mapped from the boiler-scale CFD solution at a plane intersecting SH2 at the corresponding position, while the effective thermophysical and radiative properties of the flue-gas mixture are determined from the boiler-scale simulation results;
- Wall temperatures at lateral boundaries and the roof are prescribed based on boiler operating data and heat balance considerations;
- Steam inlet conditions (temperature and mass flow rate) in each tube are taken from the one-dimensional Aspen HYSYS model described in Section 2.2.

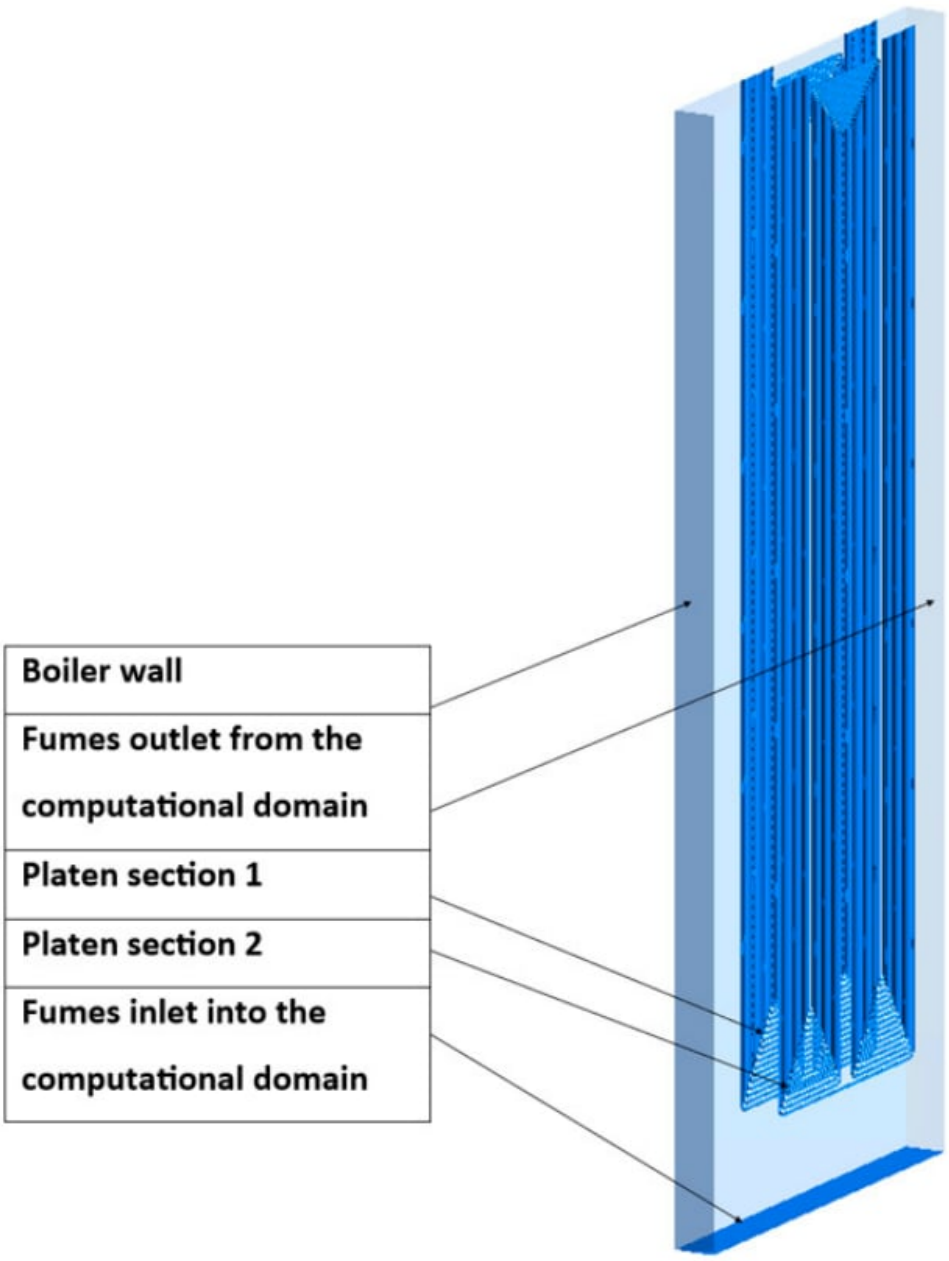


Figure 6. Schematic view of the computational domain used in the detailed CFD model of the SH2 fragment.

With these inputs, the SH2 fragment model solves for the gas-side flow and temperature fields around the tubes, the steam-side flow and temperature inside the tubes, and the three-dimensional tube metal temperature distribution.

2.4.3. Physical and Numerical Models Used in the SH2 Fragment Simulations

The SH2 fragment was modelled in ANSYS CFX using three adjacent computational domains solved in parallel: a flue-gas domain, a solid tube-wall domain and a steam domain inside the tubes. Heat transfer between the domains was represented by exchanging temperatures and heat fluxes at the common interfaces, so that the gas, metal and steam regions form a conjugate heat-transfer system. This arrangement makes it possible to apply appropriate physical models and operating pressures for each medium and at the same time limits numerical diffusion related to the large pressure difference between the high-pressure steam in the tubes (about 13.5 MPa) and the flue gas outside (close to atmospheric pressure).

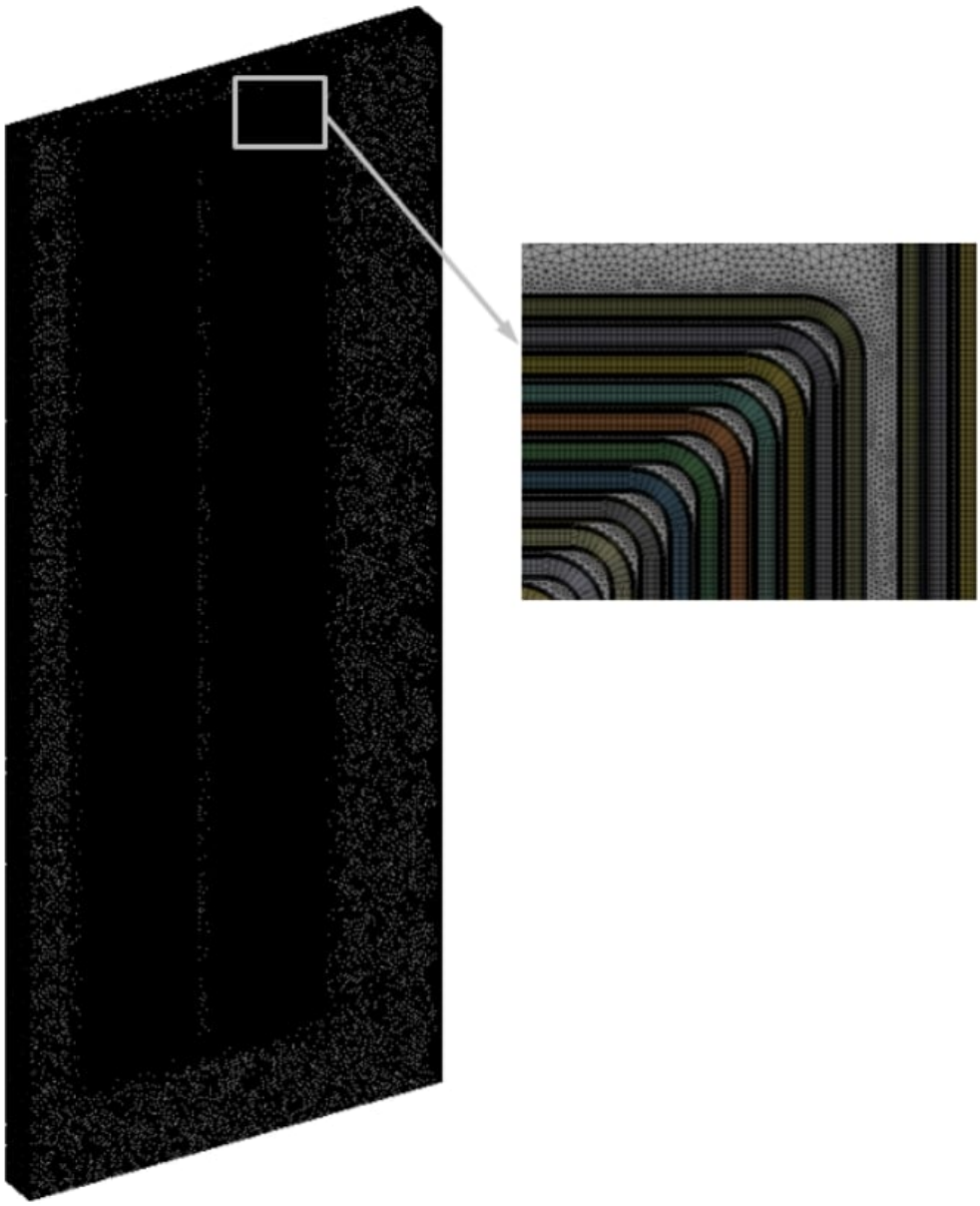


Figure 7. Numerical mesh used in the detailed CFD model of the SH2 fragment—overall view and a close-up of the tube bundle region.

The flue gas was represented as a homogeneous equivalent gas rather than by individual chemical species. The air material definition available in ANSYS CFX was used as a starting point, and its molar mass, specific heat capacity, dynamic viscosity, thermal conductivity, and radiative properties were adjusted based on the effective properties of the flue-gas mixture obtained from the boiler-scale simulations. The equivalent gas was treated as an ideal gas, with gravity included to account for buoyancy. Turbulence was represented using a k–ε model [25,39]. Because the modelled region is located downstream of the combustion zone, no combustion model was activated. Radiative heat transfer was taken into account with the Discrete Transfer radiation model [40,41]. At the gas inlet, flow parameters obtained from the boiler-scale CFD simulations were imposed, and on the remaining part of the inlet surface, a boundary condition was applied to represent radiation incoming from the hotter furnace chamber.

The tube-wall domain was treated as a solid region with material properties corresponding to the tube steel, defined by density, specific heat capacity and thermal conductivity. This

allowed heat conduction through the tube walls to be resolved and provided the thermal link between gas and steam.

In the steam domain, water (gas) was used as the working fluid with an operating pressure of 13.5 MPa. Radiative heat transfer was not considered in this region. Turbulence in the steam flow was modelled with a k–ε model [42]. Inlet steam conditions (mass flow rate and temperature for each tube) were taken from the one-dimensional Aspen HYSYS model described in Section 2.2, and the outlet pressure was set consistently with the operating point of the water–steam cycle. Only single-phase steam flow was considered inside the tubes.

3. Results

3.1. 1D Model of Platen Steam Superheater

The one-dimensional model was applied to illustrate how the proposed modelling approach can be used under example boiler conditions. Boundary conditions were taken from design and operating data for the unit. These simulations serve as benchmark points for verifying the consistency of the 1D model with available reference calculations.

The pressure drop over the tubes was stabilised at approximately 182.0 kPa. Figure 8 presents the distribution of steam mass flow rate among the tubes. Although the overall mass flow rate is evenly distributed, noticeable deviations from the mean value can be identified for individual tubes. These deviations are a direct consequence of geometric differences and varying local pressure losses within the platen. The obtained mass flow rate distribution confirms the necessity of accounting for tube-level flow maldistribution when analysing the thermal and hydraulic performance of the superheater. The highest mass flow rate was observed for tube no. 1. It was caused by differences in tube geometry (Figure 6). As the first tube geometry is simpler, lower pressure drops for the same mass flow would occur. As the pressure difference for each tube should be equal, a higher mass flow rate of steam was noticed in tube no. 1. Then, the lowest mass flow rate was observed in tube no. 2. It is the longest pipe, with complex geometry, so the share of geometrically caused pressure drops is the highest, causing the need for a mass flow rate decrease to equalise the pressure drops. For tubes 3–16, mass flow increases as the tube length decreases, although discrepancies between them are not so significant.

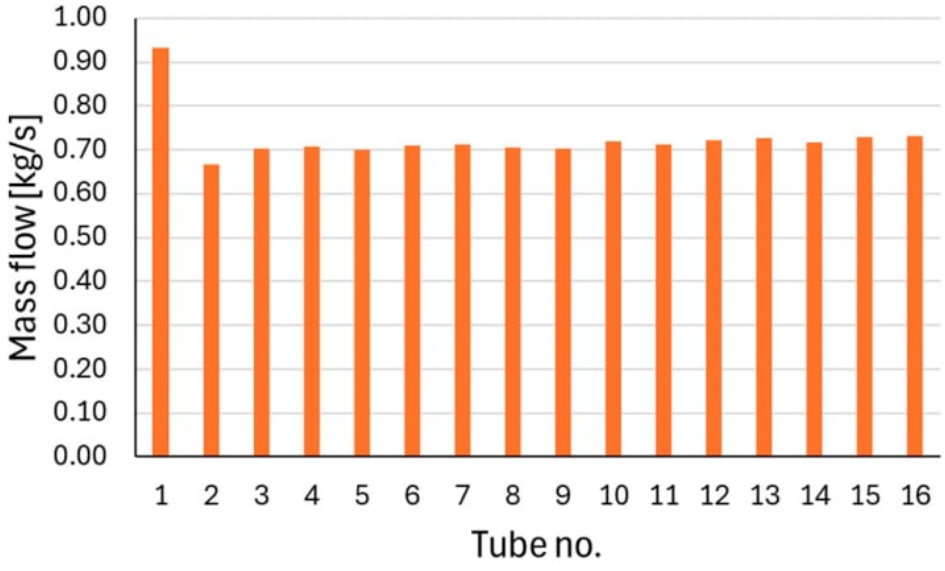


Figure 8. Distribution of steam mass flow rate among the tubes of the analysed platen for the reference full-load operating point.

3.2. Boiler-Scale CFD: Gas-Side Thermal Conditions

The boiler-scale CFD simulation for the nominal operating point provides three-dimensional gas-side boundary conditions for the superheater region. The calculated fields of temperature, pressure and oxygen mass fraction on selected horizontal planes are shown in Figure 9.

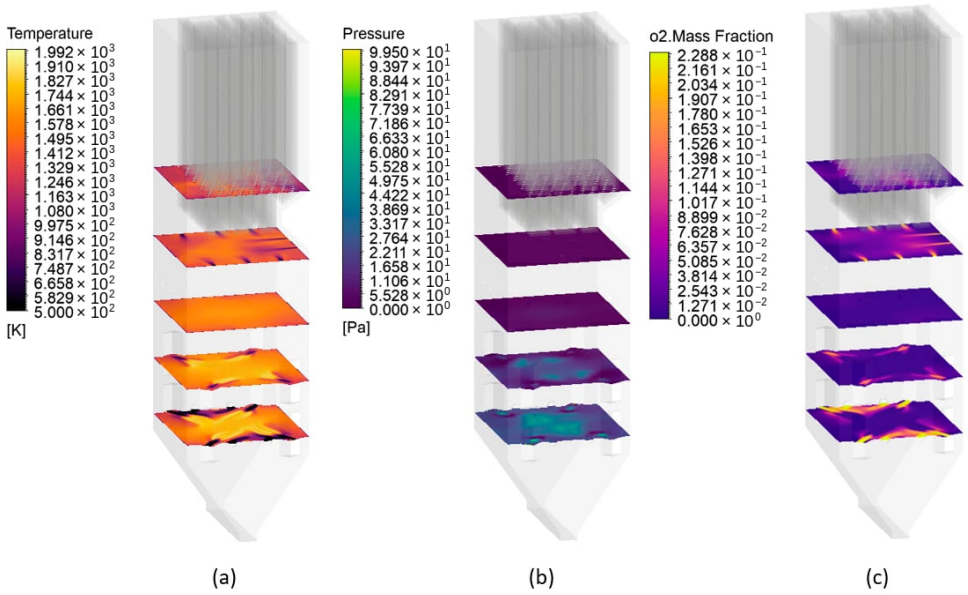


Figure 9. Boiler-scale CFD results at selected horizontal planes: (**a**) gas temperature, (**b**) static pressure, and (**c**) oxygen mass fraction.

These results characterise the thermal and flow conditions in the first pass of the boiler and provide the basis for defining boundary conditions for the SH2 fragment model. The calculated distributions show the spatial variation in the gas temperature and composition in the furnace region and indicate the thermal environment to which the platen superheater is exposed under nominal load.

3.3. Superheater Numerical Model Results

The SH2 fragment CFD model combines gas-side boundary conditions obtained from the boiler-scale simulation with steam-side inlet data taken from the one-dimensional HYSYS model. By solving the coupled heat-transfer problem in the flue-gas, tube-wall and steam domains, the model provides three-dimensional distributions of flue-gas temperature, tube metal temperature and steam temperature in the analysed superheater region.

Representative results of the SH2 fragment simulation are shown in Figure 10, which presents the flue-gas temperature in a plane passing through the upper part of the superheater, the tube metal temperature, and the steam temperature at the outlet from the superheater tubes. The calculated outer wall temperature distribution in the lower horizontal part of one of the platens is shown separately in Figure 11.

The results indicate clear temperature differences between individual tube locations and between particular parts of the platen geometry. These distributions reflect the combined influence of local gas-side thermal conditions, heat conduction through the tube walls and steam-side cooling conditions. The calculated temperature field shows a wide variation in both the tube metal and steam temperatures within the analysed superheater fragment. The tube metal temperature ranged from 652.5 K to 1008 K. The minimum value was close to the inlet steam temperature, whereas the maximum value was found in the region exposed to radiation from the furnace chamber. The steam temperature varied from 652.1 K at the inlet to

a maximum of 850.7 K inside the superheater. The distribution of average steam temperatures at the outlets of the individual superheater tubes is presented in Figure 12.

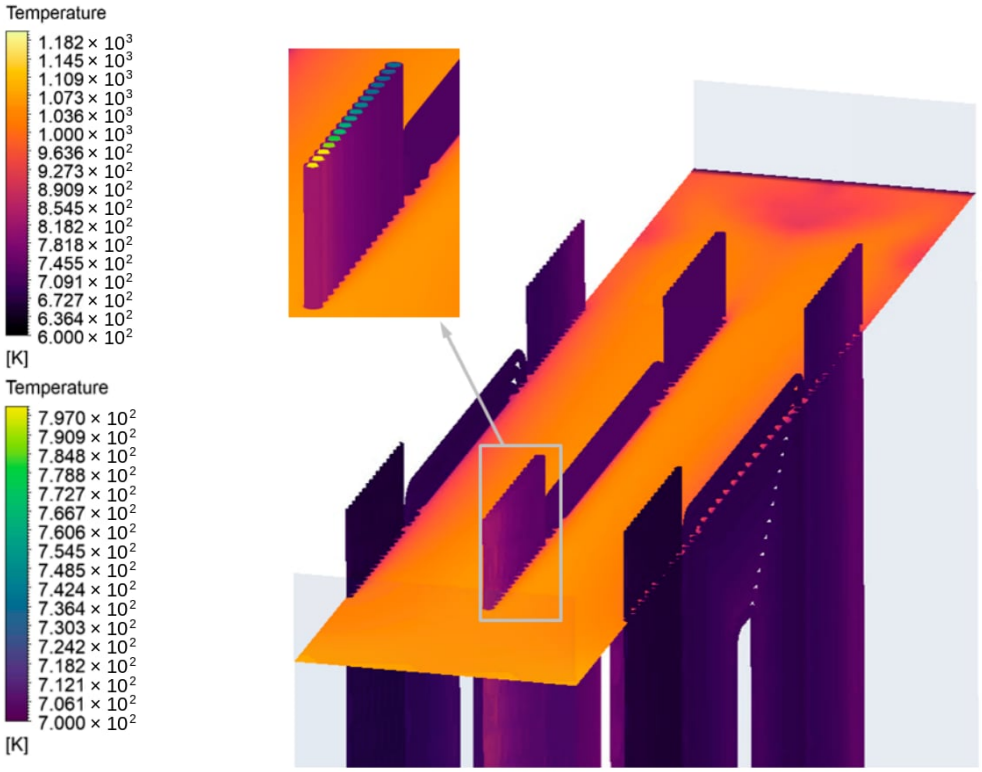


Figure 10. CFD calculation results for the superheater: exhaust gas temperature at the plane passing through the upper part of the superheater (temperature scale—(**upper left**)), metal temperature of the tubes (temperature scale—(**upper left**)), and steam temperature at the outlet from the superheater tubes (temperature scale—(**bottom left**)).

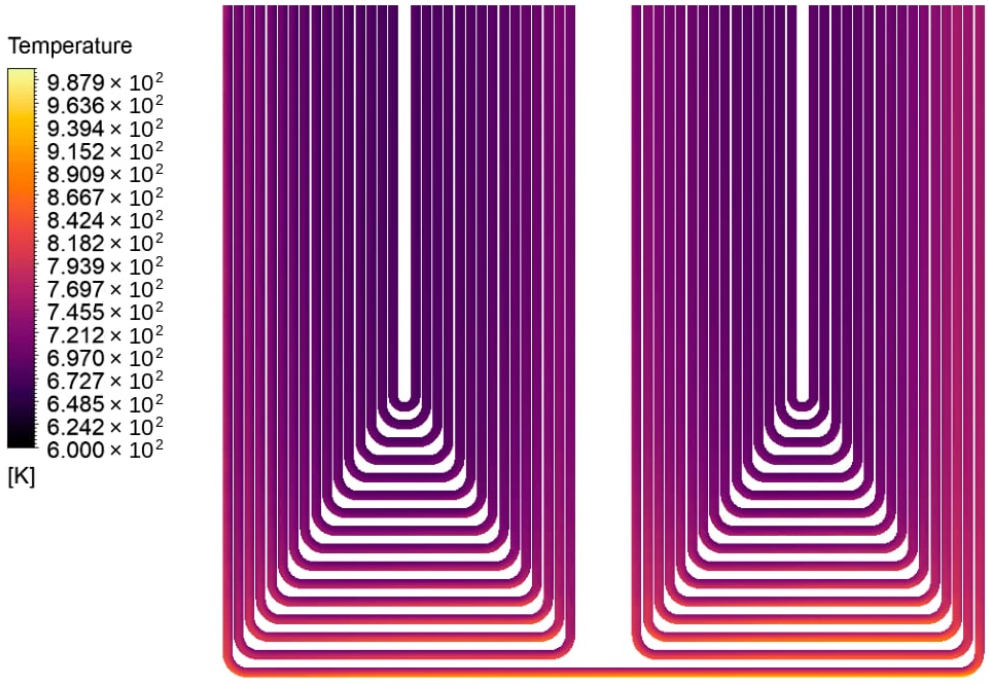


Figure 11. Outer tube wall temperature distribution in the lower horizontal part of the analysed SH2 platen obtained from the SH2 fragment CFD simulation.

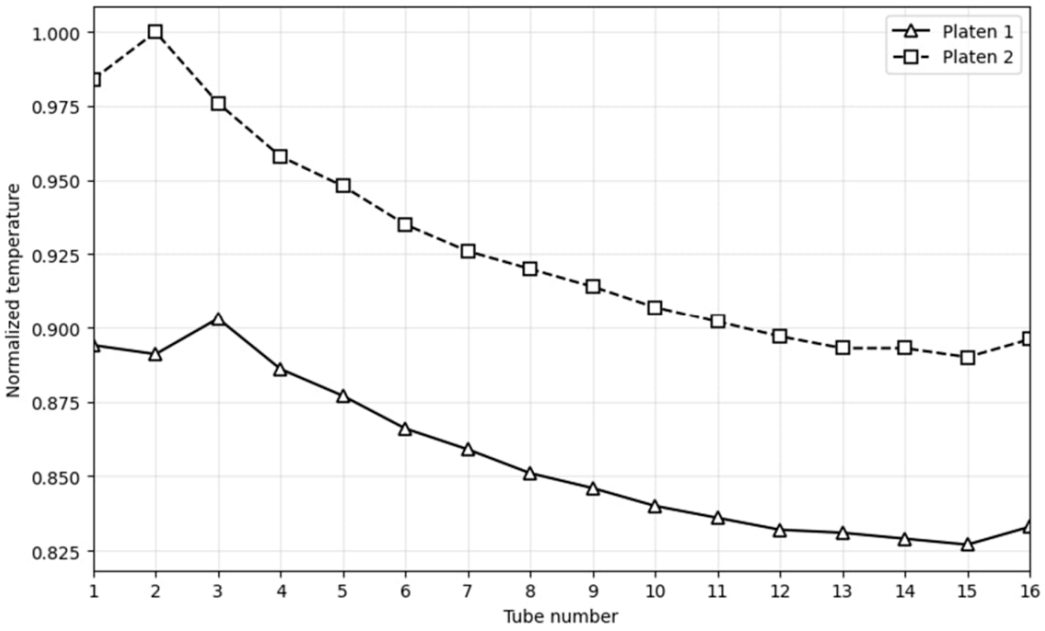


Figure 12. Normalised outlet steam temperature in individual tubes of Platen 1 and Platen 2.

By solving the coupled flow and heat-transfer problem, the model predicts three-dimensional tube wall temperature fields for the analysed platens. An example of the calculated outer wall temperature distribution in the lower horizontal part of one of the platens is presented in Figure 11. The obtained distributions show clear differences between tube locations and between horizontal and vertical segments, reflecting the combined influence of gas-side exposure, steam-side conditions and tube geometry. From a modelling point of view, these results demonstrate the capability of the proposed CFD framework to identify regions of elevated tube temperature and to provide quantitative data suitable for subsequent mechanical or lifetime assessments.

As shown in Figure 12, the normalised outlet steam temperature is systematically higher in Platen 2 than in Platen 1 over the entire range of tube numbers. The highest values are observed for the first tubes, and then a gradual decrease is visible toward the outer part of each platen, with a slight rise again for the last tube. The higher temperature level observed in Platen 2 can be attributed to its location closer to the central region of the boiler, where the tubes are more strongly exposed to radiation from the furnace chamber and to higher flue-gas temperatures. As a result, the steam leaving the tubes of Platen 2 reaches consistently higher temperatures than in the corresponding tubes of Platen 1.

4. Discussion

The results obtained in this study confirm that the thermal and hydraulic behaviour of a radiant platen superheater is difficult to represent accurately using a single modelling approach alone, as also indicated in the literature. The 1D model, the boiler-scale CFD model, and the detailed conjugate CFD model each capture different aspects of the physical problem, and their integration provides a more complete representation of the operating conditions of SH2 than any standalone method. Moreover, the proposed framework remains computationally tractable while providing stable numerical solutions.

Previous studies have demonstrated the potential of coupled CFD–1D approaches for predicting non-uniform thermal loading and steam flow distribution in boiler superheaters, as well as the application of three-dimensional conjugate heat-transfer models for detailed analysis of local tube temperatures. Building on these developments, the distinguishing feature of the present study is the integration of three complementary modelling approaches:

a one-dimensional thermo-hydraulic model of steam flow in individual tubes, a boiler-scale CFD model providing spatially resolved flue-gas conditions, and a detailed three-dimensional conjugate heat-transfer model of the SH2 fragment. Importantly, the latter explicitly resolves three coupled three-dimensional computational domains representing the flue gas, the solid tube walls, and the steam flowing inside the tubes. This enables the simultaneous consideration of non-uniform gas-side thermal loading, heat conduction through the tube walls, and tube-specific steam-side cooling conditions. Consequently, the proposed framework provides a detailed representation of local tube metal temperature distributions while limiting the computationally demanding three-dimensional analysis to the selected superheater fragment. This multi-scale approach offers a practical methodology for identifying regions susceptible to local overheating under industrial boiler operating conditions [43–45]. The 1D thermo-hydraulic model proved particularly useful for resolving the steam-side flow distribution among individual tubes of the analysed platen. The calculations showed measurable maldistribution of steam mass flow rate between tubes. This effect results mainly from differences in tube geometry and associated hydraulic resistance. The first tube, characterised by the simplest flow path, carried the highest steam mass flow rate, whereas the second tube, being the longest and geometrically most complex, exhibited the lowest flow rate. Although these differences are not extreme, they are thermally relevant because local reductions in steam flow directly weaken convective cooling on the internal tube surface, increasing susceptibility to metal overheating. This observation is consistent with previous findings reported in the literature, where flow maldistribution was identified as one of the key mechanisms governing non-uniform wall temperatures in platen and pendant superheaters.

The boiler-scale CFD model complemented the 1D analysis by providing spatially resolved gas-side thermal conditions in the first pass of the boiler. The predicted temperature and flue-gas distributions revealed the non-uniform thermal environment in which the SH2 superheater operates. This is important because radiant platen surfaces are exposed to strongly position-dependent heat loads resulting from furnace aerodynamics, combustion intensity, and radiative heat flux. In simplified engineering models, such effects are usually represented by averaged or assumed heat fluxes, which may be sufficient for overall heat balance calculations but are not adequate for identifying local thermal extremes. In the present approach, the CFD-derived gas-side fields served as a physically justified basis for defining boundary conditions for the local superheater model.

The detailed CFD model of the SH2 fragment provided the highest level of local resolution and allowed the coupled analysis of flue gas, tube walls, and steam. The results demonstrated that the wall temperature distribution is inherently three-dimensional and depends on several factors: the local gas temperature field, radiative and convective heat-transfer conditions, steam-side mass flow rate, and the geometric arrangement of the tubes. Elevated wall temperatures were observed in regions exposed to stronger thermal loading and less favourable cooling conditions. The lower horizontal part of the platen appears particularly important in this respect, which is physically consistent with the expected thermal exposure of this region in a radiant superheater. These findings confirm that the proposed framework is capable of identifying locations potentially critical from the standpoint of material durability.

An important outcome of the study is the demonstration that iterative coupling between models significantly improves the consistency of the simulation framework. The 1D model alone can estimate steam temperatures and pressure drops, but it cannot independently determine the actual spatial distribution of external heat load. Conversely, CFD analysis of the gas side alone cannot reproduce realistic steam-side redistribution effects without additional information about the internal flow conditions. The present methodology overcomes

this limitation by linking the models through exchanged boundary conditions. As a result, both the gas-side and steam-side descriptions become more physically representative.

From a practical point of view, the proposed approach offers a compromise between computational cost and modelling detail. Full-scale conjugate CFD simulation of the entire boiler together with explicitly resolved internal steam flow in all superheater tubes would be prohibitively expensive for engineering applications. In contrast, the present framework uses the boiler-scale CFD model only where large-scale furnace processes must be captured, applies the 1D model where rapid and robust steam-side calculations are sufficient, and reserves the high-resolution CFD analysis for the selected superheater fragment where local metal temperatures are of greatest interest. This decomposition makes the approach suitable for design support, diagnostic studies, and sensitivity analyses under different operating conditions.

The developed methodology constitutes a robust basis for further model development. In particular, the framework can be extended toward transient analyses, inclusion of ash fouling resistance, and coupling with thermo-mechanical calculations for stress and lifetime assessment. Such extensions would further increase its industrial relevance, especially for preventive diagnostics and optimisation of superheater operation.

5. Conclusions

This study presented a modelling framework for the analysis of a radiant platen superheater operating under industrial boiler conditions. The proposed approach combines a one-dimensional steam-side model, a boiler-scale CFD model, and a detailed conjugate CFD model of a selected superheater fragment. On the basis of the obtained results, the following conclusions can be drawn:

1. The 1D model reproduced the non-uniform steam flow distribution among individual tubes of the analysed platen and demonstrated that tube geometry and local hydraulic resistance affect flow maldistribution and pressure-drop equalisation.
2. The boiler-scale CFD model provided spatially resolved gas-side boundary conditions, revealing non-uniformity of the thermal environment in the superheater region that cannot be captured by simplified averaged approaches.
3. The detailed SH2 fragment CFD model enabled the prediction of three-dimensional distributions of flue-gas temperature, steam temperature, and tube metal temperature, making it possible to identify locally overheated regions of the platen.
4. The coupling of the 1D and CFD models improved the physical consistency of the analysis by accounting simultaneously for steam-side flow redistribution and gas-side non-uniform thermal loading.
5. The developed methodology offers a practical compromise between modelling accuracy and computational cost, and therefore constitutes a useful engineering tool for radiant heat exchanger analysis, operational diagnostics, and support of design decisions.

Future work should focus on extending the framework to multiple operating conditions, as well as incorporating fouling effects and thermo-mechanical analysis in order to support lifetime prediction and integrity assessment of superheater components.

Author Contributions: M.K.-G.: Conceptualisation, methodology, software, investigation, data curation, visualisation, writing—original draft preparation, writing—reviewing and editing. A.D.: methodology, data curation, writing—original draft preparation, writing—reviewing and editing. A.K.: software, data curation. P.P.: writing—original draft preparation. J.Z.: conceptualisation, project administration. P.K.: conceptualisation, methodology, investigation, project administration, supervision. All authors have read and agreed to the published version of the manuscript.

Funding: This research received no external funding.

Data Availability Statement: The raw data supporting the conclusions of this article will be made available by the authors on request.

Conflicts of Interest: Author Jolanta Ziaja was employed by the company Grupa Kapitałowa Polimex Mostostal. The remaining authors declare that the research was conducted in the absence of any commercial or financial relationships that could be construed as a potential conflict of interest.

References

1. Chen, X.; Zhong, W.; Li, T. Fast prediction of temperature and chemical species distributions in pulverized coal boiler using POD reduced-order modeling for CFD. *Energy* **2022**, *276*, 127663. [CrossRef]
2. González, M.M.P.; García, F.J.F.; Ramón, I.S.; Roces, H.S. Experimental thermal behavior of a power plant reheater. *Energy* **2006**, *31*, 665–676. [CrossRef]
3. Jin, D.; Yan, J.; Liu, X.; Zhang, C.; Wang, H. Prediction of tube temperature distribution of boiler platen superheater by a coupled combustion and hydrodynamic model. *Energy* **2023**, *279*, 128116. [CrossRef]
4. Modliński, N.; Szczepanek, K.; Nabagło, D.; Madejski, P.; Modliński, Z. Mathematical procedure for predicting tube metal temperature in the second stage reheater of the operating flexibly steam boiler. *Appl. Therm. Eng.* **2019**, *146*, 854–865. [CrossRef]
5. Madejski, P.; Taler, D. Analysis of temperature and stress distribution of superheater tubes after attemperation or sootblower activation. *Energy Convers. Manag.* **2013**, *71*, 131–137. [CrossRef]
6. Madejski, P.; Taler, D.; Taler, J. Numerical model of a steam superheater with a complex shape of the tube cross section using Control Volume based Finite Element Method. *Energy Convers. Manag.* **2016**, *118*, 179–192. [CrossRef]
7. Edge, P.J.; Heggs, P.J.; Pourkashanian, M.; Stephenson, P.L. Integrated fluid dynamics-process modelling of a coal-fired power plant with carbon capture. *Appl. Therm. Eng.* **2013**, *60*, 242–250. [CrossRef]
8. Shen, Y.; Guo, B.; Yu, A.; Maldonado, D.; Austin, P.; Zulli, P. Three-dimensional modelling of coal combustion in blast furnace. *ISIJ Int.* **2008**, *48*, 777–786. [CrossRef]
9. Xu, M.; Azevedo, J.L.T.; Carvalho, M.G. Modeling of a front wall fired utility boiler for different operating conditions. *Comput. Methods Appl. Mech. Eng.* **2001**, *190*, 3581–3590. [CrossRef]
10. Prieto, M.M.; Suárez, I.; Fernández, F.J.; Sánchez, H.; Mateos, M. Theoretical development of a thermal model for the reheater of a power plant boiler. *Appl. Therm. Eng.* **2007**, *27*, 619–626. [CrossRef]
11. Prieto, M.M.; Suárez, I.; Fernández, F.J.; Sánchez, H.; Viescas, C. Application of a thermal model to a power plant reheater with irregular tube temperatures. *Appl. Therm. Eng.* **2007**, *27*, 185–193. [CrossRef]
12. Modlinski, N. Computational modeling of a utility boiler tangentially-fired furnace retrofitted with swirl burners. *Fuel Process. Technol.* **2010**, *91*, 1601–1608. [CrossRef]
13. Park, H.Y.; Faulkner, M.; Turrell, M.D.; Stopford, P.J.; Kang, D.S. Coupled fluid dynamics and whole plant simulation of coal combustion in a tangentially-fired boiler. *Fuel* **2010**, *89*, 2001–2010. [CrossRef]
14. Duda, P. Inverse estimation of the transient-state stress distribution in the power boiler pressure components. *Int. J. Mech. Sci.* **2016**, *107*, 201–214. [CrossRef]
15. Fu, J.; Liu, Z.; Wei, L.; Lin, L.; Li, N.; Zhou, Q.; Ma, C. Identification of the running status of membrane walls in an opposed fi red model boiler under varying heating loads. *Appl. Therm. Eng.* **2019**, *173*, 2020. [CrossRef]
16. Laubscher, R.; Rousseau, P. CFD study of pulverized coal-fired boiler evaporator and radiant superheaters at varying loads. *Appl. Therm. Eng.* **2019**, *160*, 114057. [CrossRef]
17. Vessakosol, P.; Charoensuk, J. Numerical analysis of heat transfer and flow field around cross-flow heat exchanger tube with fouling. *Appl. Therm. Eng.* **2010**, *30*, 1170–1178. [CrossRef]
18. Song, G.; Qi, X.; Yang, S.; Yang, Z. Investigation of ash deposition and corrosion during circulating fl uidized bed combustion of high-sodium, high-chlorine Xinjiang lignite. *Fuel* **2017**, *214*, 207–214. [CrossRef]
19. Dzido, A.; Wo, M.; Krawczyk, P. Transcritical carbon dioxide cycle as a way to improve the efficiency of a Liquid Air Energy Storage system. *Renew. Energy* **2022**, *196*, 1385–1391. [CrossRef]
20. Igbagbon, E.J.; Orhorhoro, E.K.; Erhinyodavwe, O. Design Analysis of a Miniature Steam Boiler for the Generation of Steam. *J. Sci. Tech. Resear.* **2024**, *6*, 87–98.
21. Meyer, C.A.; McClintock, R.B.; Silvestri, G.J.; Spencer, R.C. *Thermodynamic and Transport Properties of Steam*; The American Society of Mechanical Engineers: New York, NY, USA, 1967.
22. AspenTech Documentation Team. HYSYS ® 2004.2 Simulation Basis. In *AspenTech Software Manual*; Aspen Technology, Inc.: Cambridge, MA, USA, 2005; pp. 46–52.
23. *Aspen HYSYS—Operations Guide*; Aspen Technology, Inc.: Cambridge, MA, USA, 2018.
24. Tony, M.S.K.; Utomo, S.; Nurrochim, W.F.; Harmoko, U. Monoblock Geothermal Power Plant Assessment in Geothermal Working Area Dieng. *Eng. Environ. Sci.* **2024**, *4*, 314–325. [CrossRef]

25. Shih, T.-H.; Liou, W.W.; Shabbir, A.; Yang, Z.; Zhu, J. A New k-ε Eddy Viscosity Model for High Reynolds Number Turbulent Flows. *Comput. Fluids* **1995**, *24*, 227–238. [CrossRef]
26. Ji, C.-C.; Cohen, R.D. An investigation of the combustion of pulverized coal-air mixture in different combustor geometries. *Combust. Flame* **1992**, *90*, 307–343. [CrossRef]
27. Xie, Y.; Liu, X.; Zhang, C.; Zhao, J.; Wang, H. Coupled heat transfer model for the combustion and steam characteristics of coal-fired boilers. *Eng. Appl. Comput. Fluid Mech.* **2021**, *15*, 490–502. [CrossRef]
28. Benim, A.C.; Deniz Canal, C.; Boke, Y.E. Computational investigation of oxy-combustion of pulverized coal and biomass in a swirl burner. *Energy* **2022**, *238*, 121852. [CrossRef]
29. Silva, C.V.; Dondoni, L.F.; Ermel, C.; Bellani, P.L.; Stradioto, D.A.; Indrusiak, M.L.S. CFD analysis of the combustion process in a boiler of a 160 MWe power plant: Leakage influence. *J. Braz. Soc. Mech. Sci. Eng.* **2019**, *41*, 287. [CrossRef]
30. Raithby, G.D.; Chui, E.H. A Finite-volume Method for Predicting a Radiant Heat Transfer in Enclosures with Participating Media. *J. Heat Transfer.* **1990**, *112*, 415–423. [CrossRef]
31. Chui, E.H.; Raithby, G.D. Computation of radiant heat transfer on a nonorthogonal mesh using the finite-volume method. *Numer. Heat Transf.* **1993**, *23*, 269–288. [CrossRef]
32. Zhang, H.; Lin, H.; Zhou, X.; Wang, X.; Zheng, H.; Liu, Y.; Tan, H. CFD modeling and industry application of a self-preheating pulverized coal burner of high coal concentration and enhanced combustion stability under ultra-low load. *Appl. Therm. Eng.* **2024**, *253*, 123831. [CrossRef]
33. Hernik, B. Numerical Research of Flue Gas Denitrification Using the SNCR Method in an OP 650 Boiler. *Energies* **2022**, *15*, 3427. [CrossRef]
34. Magnussen, B.F.; Hjertager, B.H. On mathematical modeling of turbulent combustion with special emphasis on soot formation and combustion. In *Symposium (International) on Combustion*; Elsevier: Amsterdam, The Netherlands, 1977; pp. 719–729.
35. Fang, K.; Zhang, D.; Wang, D.; Liu, Z.; Zhang, M.; Zhang, S. The impact of coal gasification slag powder on fluidity, rheology and viscoelasticity properties of fresh cement paste. *J. Build. Eng.* **2022**, *69*, 106237. [CrossRef]
36. Li, C.; Zhang, Z.; Feng, D.; Wang, Y.; Wang, Y.; Zhao, Y.; Guo, X.; Sun, S. Transient CFD Analysis of Combustion and Heat Transfer in a Coal-Fired Boiler Under Flexible Operation. *Energies* **2026**, *19*, 478. [CrossRef]
37. Li, L.; Jiang, B.; Wei, G.; Li, X.; Zhu, Z. Multiscale multiphase flow simulations using interface capturing and Lagrangian particle tracking. *Phys. Fluids* **2022**, *34*, 121801. [CrossRef]
38. Mangani, L.; Casartelli, E.; Darwish, M. Coupled pressure based CFD solver for turbomachinery flows: Overview of applications. In Proceedings of the 13th European Conference on Turbomachinery Fluid Dynamics & Thermodynamics, Lausanne, Switzerland, 8–12 April 2019; pp. 1–10. [CrossRef]
39. ANSYS. ANSYS FLUENT Theory Guide. *Knowl. Creat. Diffus. Util.* **2010**, *15317*, 724–746.
40. Baburic, M.; Raulot, A.; Coelho, P.J.M.; Duic, N. Application of the conservative discrete transfer radiation method to a furnace with complex geometry. In *CHT-04-Advances in Computational Heat Transfer III. Proceedings of the Third International Symposium, Berkeley, CA, USA, 26–27 April 2004*; Begel House Inc.: Danbury, CT, USA, 2004.
41. Lockwood, F.C.; Shah, N.G. A new radiation solution method for incorporation in general combustion prediction procedures. In *Symposium (International) on Combustion*; Elsevier: Amsterdam, The Netherlands, 1981; pp. 1405–1414.
42. Lertanan, T.; Podjanasatja, V.; Chuchan, D.; Sukjai, Y. Investigating the Characteristics of Pulverized Coal Combustion Using Ansys Fluent: A CFD Study of a 300 kW Swirl Burner. *J. Combust.* **2024**, *2024*, 3128387. [CrossRef]
43. Radhakrishnan, K.; Park, J.S. Flow and Heat Transfer Characteristics of Superheater Tube of a Pulverized Coal-Fired Boiler Using Conjugate Heat Transfer Modeling. *Energies* **2024**, *17*, 1161. [CrossRef]
44. Laubscher, R.; Rousseau, P. Coupled simulation and validation of a utility-scale pulverized coal-fired boiler radiant final-stage superheater. *Therm. Sci. Eng. Prog.* **2020**, *18*, 100512. [CrossRef]
45. Granda, M.; Trojan, M.; Taler, D.; Grądziel, S.; Dzierwa, P.; Kaczmarski, K.; Sobota, T. A hybrid approach to CFD modeling of the combustion chamber and the platen superheater. *Fuel* **2026**, *409*, 137707. [CrossRef]

Disclaimer/Publisher's Note: The statements, opinions and data contained in all publications are solely those of the individual author(s) and contributor(s) and not of MDPI and/or the editor(s). MDPI and/or the editor(s) disclaim responsibility for any injury to people or property resulting from any ideas, methods, instructions or products referred to in the content.